



Martingale Problem on Random Manifolds

Existence of the Martingale Problem on Random Manifolds

Giorgio Micaletto

Bocconi University

May 25, 2025

Roadmap

- 1 Motivation
- 2 Prelude: What is a Martingale?
- 3 A Gentle Tour of Manifolds
- 4 A Deeper Dive in Random Manifolds
- 5 Existence of the Martingale Problem
- 6 Appendix: Pathwise Existence and Uniqueness

B

Why Random Manifolds? From Euclidean Space to Uncertain Geometry

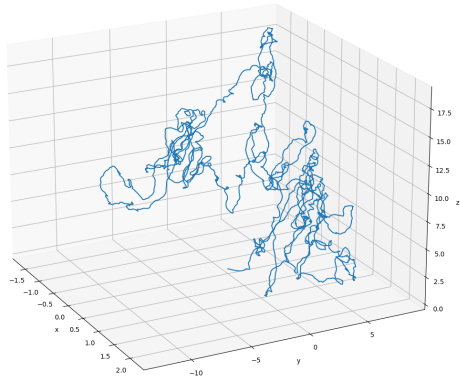
- Classical stochastic processes live in \mathbb{R}^d ; geometry is flat and deterministic.
- Applications increasingly involve *uncertain* or *curved* environments.
- Random geometry appears in biology, physics, data science, and engineering (examples on next slides).
- Need: a generator-based framework stable under geometric randomness \Rightarrow the martingale problem.

Martingales 101

Definition (Discrete Time)

A sequence $(M_n)_{n \geq 0}$ adapted to a filtration (\mathcal{F}_n) is a *martingale* if $\mathbb{E}[|M_n|] < \infty$ and $\mathbb{E}[M_{n+1} | \mathcal{F}_n] = M_n$ almost surely.

- "Fair game" property: current value is best prediction of future.
- Continuous-time analogue: (M_t) s.t. $\mathbb{E}[M_t | \mathcal{F}_s] = M_s$ for $s \leq t$.
- Examples: Brownian motion B_t , compensated Poisson process $N_t - \lambda t$.



Why Martingales Matter for Diffusions

- For a diffusion X_t with generator \mathcal{A} , *all* f in the domain yield martingales

$$f(X_t) - f(X_0) - \int_0^t \mathcal{A}f(X_s) \, ds.$$

- Conversely, specifying the class of martingales pins down the law of X_t (Stroock–Varadhan).
- Unifies Itô calculus, potential theory, and PDE methods.

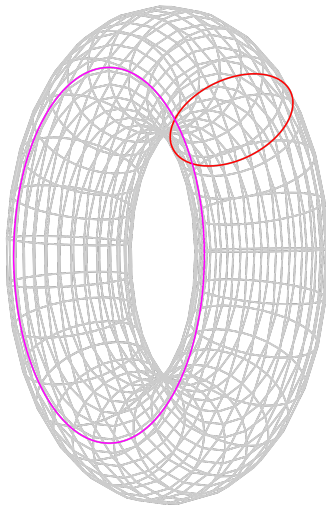
Key takeaway: Martingale problems translate stochastic dynamics into analytic conditions.

From Curves and Surfaces to Higher-Dimensional Manifolds

We build intuition in three familiar steps:

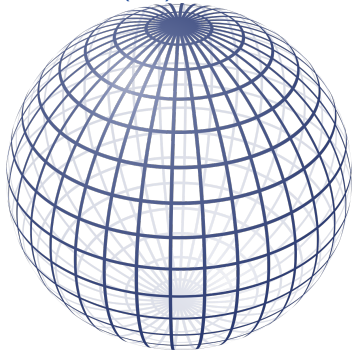
- ① **Curves (1-D)**: A thin wire in \mathbb{R}^2 —zoom in and it looks like a straight line.
- ② **Surfaces (2-D)**: The Earth's surface in \mathbb{R}^3 —up close it is nearly flat like a sheet of paper.
- ③ **General d** : A space \mathcal{M} is a *d -manifold* if every point has a neighbourhood smoothly matching \mathbb{R}^d .

Charts convert these local “flat views” into coordinates, and an *atlas* of charts stitches them together smoothly. Typical example (shown on the right) is the torus \mathcal{T}^2 .

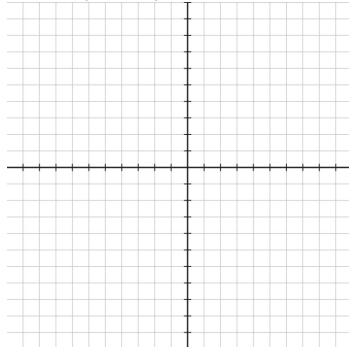


Curvature in Three Pictures

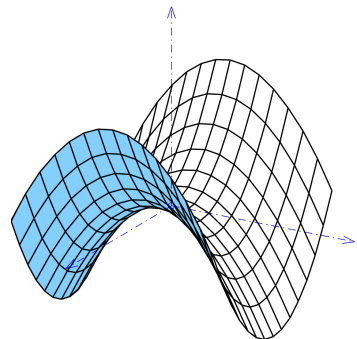
Positive (S^2)



Zero (plane)



Negative (saddle)



Curvature controls how diffusions spread and how heat dissipates on \mathcal{M} .

B

Tangent Spaces and the Riemannian Metric

- At $p \in \mathcal{M}$, the *tangent space* $T_p\mathcal{M}$ collects velocities of curves through p .
- The metric tensor g on \mathcal{M} is a function that assigns to each point $p \in \mathcal{M}$ a symmetric, positive-definite bilinear form

$$g_p : T_p\mathcal{M} \times T_p\mathcal{M} \rightarrow \mathbb{R},$$

This means that at each point $p \in \mathcal{M}$, the metric tensor g_p provides an inner product on the tangent space $T_p\mathcal{M}$. The smoothness condition ensures that the metric varies smoothly across the manifold.

In a local coordinate chart (U, φ) on \mathcal{M} , where $\varphi : U \rightarrow \mathbb{R}^n$ assigns coordinates (x^1, x^2, \dots, x^n) to points in U , the metric tensor can be expressed in terms of its components relative to the coordinate basis. The coordinate functions induce a basis for the tangent space $T_p\mathcal{M}$ at each point $p \in U$, given by the partial derivative vectors

$$\left\{ \frac{\partial}{\partial x^i} \Big|_p \right\}_{i=1}^n.$$

Useful Differential Operators

- ∇ (gradient). For a function f on a manifold \mathcal{M} with metric g ,

$$\nabla f := g^{ik} \frac{\partial f}{\partial x^k} e_i.$$

- div (the divergence) defined as

$$\operatorname{div}_g V := \frac{1}{\sqrt{|g|}} \frac{\partial}{\partial x^i} \left(\sqrt{|g|} V^i \right)$$

for a vector field V , where $|g| = \det(g_{ij})$.

- Δ_g (the Laplace–Beltrami) defined as

$$\Delta f := \operatorname{div}_g(\nabla f),$$

i.e.

$$\Delta f = \frac{1}{\sqrt{|g|}} \frac{\partial}{\partial x^i} \left(\sqrt{|g|} g^{ij} \frac{\partial f}{\partial x^j} \right).$$

Formal Definition of Random Manifolds

Setup

Fix a probability space $(\Omega, \mathcal{F}, \mathbb{P})$. A *random manifold* is a measurable map

$$\omega \mapsto (\mathcal{M}_\omega, p_\omega, g_\omega)$$

landing in the space Riem^* of *pointed* complete Riemannian manifolds, equipped with the *pointed Cheeger–Gromov topology*.

- **Pointed:** we remember a base-point $p_\omega \in \mathcal{M}_\omega$ so balls “around the same location” can be compared.
- **Measurability:** for every open set $U \subset \text{Riem}^*$ the event $\{\omega : (\mathcal{M}_\omega, p_\omega, g_\omega) \in U\} \in \mathcal{F}$.

Measurability and Quantitative Descriptors of Random Geometry

Given the measurable map $\omega \mapsto (\mathcal{M}_\omega, g_\omega)$ we can rigorously define:

- Expected geometric quantities, e.g. $\mathbb{E}[\text{Vol}_{g_\omega}(B_r(p_\omega))]$.
- Conditional laws of diffusions: $\mathbb{P}_{\omega,x}$ solving the martingale problem on \mathcal{M}_ω .
- Random objects *built from* \mathcal{M}_ω (heat kernels, Green's functions) as jointly measurable maps.

These will be the building blocks for pathwise analysis and weak convergence results later in the talk.

Please also note the following primary stochastic observables:

- **Volume growth exponent:** α s.t. $\text{Vol}(B_r(p)) \sim r^\alpha$ in expectation.
- **Expected curvature:** $\mathbb{E}[\text{Ric}_{g_\omega}]$ and variance control the short-time heat kernel.

Diffusions Generated by a Second-Order Operator

Fix a realisation ω of the random geometry and consider

$$\mathcal{L}_\omega f(x) = \frac{1}{2} \sum_{i,j=1}^d a_\omega^{ij}(x) \nabla_i \nabla_j f(x) + \sum_{i=1}^d b_\omega^i(x) \nabla_i f(x), \quad x \in \mathcal{M}_\omega.$$

- $a_\omega^{ij}(x)$: *Diffusion matrix* — symmetric, positive-definite:

$$a_\omega(v, v) := \sum_{i,j} a_\omega^{ij} v_i v_j.$$

- ∇_i : Covariant derivative along the i -th local coordinate; double application $\nabla_i \nabla_j f$ is the *Hessian*.
- $\frac{1}{2}$: Ensures that, when $a^{ij} = g^{ij}$, \mathcal{L}_ω coincides with the operator generating Brownian motion.
- $b_\omega^i(x)$: *Drift vector field* — deterministic push in the i -th direction.

Diffusions Generated by a Second-Order Operator

Goal

Construct a probability measure $\mathbb{P}_{\omega,x}$ on $C([0,\infty), \mathcal{M}_\omega)$ such that, for every $f \in C_c^\infty(\mathcal{M}_\omega)$,

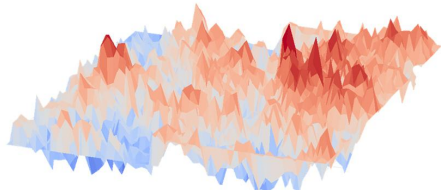
$$f(X_t) - f(X_0) - \int_0^t \mathcal{L}_\omega f(X_s) \, ds$$

is a martingale.

Why This Matters in Applications

- In option markets we observe an *implied-volatility surface* $\sigma_{\text{impl}}(k, T)$ (strike k , maturity T).
- Empirically the surface is *rougher than* a smooth sheet but still *smoother than* white noise
- Treating each daily snapshot as a *random graph* $\{(k, T, \sigma_{\text{impl}})\} \subset \mathbb{R}^3$, its geometry fluctuates with market micro-structure noise.
- Modelling σ_{impl} as a GFF supplies an explicit covariance kernel Δ^{-1} , giving closed-form risk-metrics.
- Our existence theorem ensures that under bounded-geometry assumptions there is a *martingale* price process consistent with no-arbitrage.

In all these, one needs *robust existence* as geometry jitters.



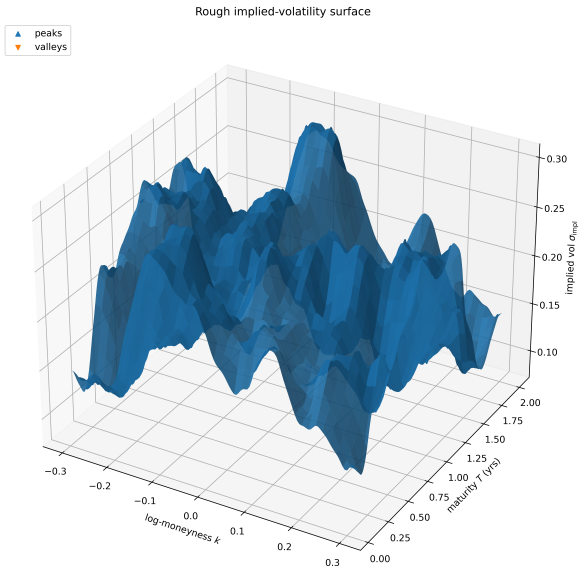
3-D render of a Gaussian Free Field

Case Study: Implied Volatility Surface as a Random Manifold

- Each trading day we observe a 2-D surface $\sigma_{\text{impl}}(k, T)$ over *log-moneyness* $k = \log(K/S_0)$ and maturity T .
- Micro-structure noise \implies surface is neither smooth nor white noise (Hurst $H \approx 0.1\text{--}0.2$).
- Model $(k, T, \sigma_{\text{impl}})$ as a random Riemannian graph

$$\mathcal{M}_\omega = \{(k, T, z) : z = \sigma_{\text{impl}}^\omega(k, T)\} \subset \mathbb{R}^3.$$

- The no-arbitrage martingale condition on the *risk-neutral* spot price process translates into a martingale problem on \mathcal{M}_ω : generator $= \frac{1}{2}\Delta_{\mathcal{M}_\omega}$ plus drift enforcing the Dupire PDE.
- Heat-kernel bounds on $\mathcal{M}_\omega \implies$ explicit VaR / X-VaR formulas and robust hedging bands.



Weak Solutions on a Random Stage

Weak Solution (in Law)

A pair $(X, \mathbb{P}_{\omega,x})$ on *some* probability space such that $X_0 = x$ a.s. and, for every $f \in C_c^\infty(\mathcal{M}_\omega)$,

$$f(X_t) - f(X_0) - \int_0^t \mathcal{L}_\omega f(X_s) \, ds$$

is a martingale.

Under *bounded geometry* this exists and is unique in law (we will prove this next slide).

Sketch of Proof — Assumptions and Step 1

Assumptions Recap

- $(\mathcal{M}_\omega, g_\omega)$ have uniform (r_0, C_k) bounded geometry.
- $\mathcal{L}_\omega = \frac{1}{2} a_\omega^{ij} \nabla_i \nabla_j + b_\omega^i \nabla_i$ with coefficients $C^{2,\alpha}$ in x and jointly measurable in ω .
- Uniform ellipticity: $\lambda^{-1} g_\omega \leq a_\omega \leq \lambda g_\omega$.

Step 1: Local Flattening

Cover \mathcal{M}_ω by normal coordinate balls $B_{r_0/2}(x_j)$ with chart maps $\varphi_{j,\omega}: B_{r_0/2}(x_j) \rightarrow \mathbb{R}^d$ whose Jacobians and derivatives are uniformly bounded by the geometry constants. In each chart the operator becomes

$$\tilde{\mathcal{L}}_{j,\omega} = \frac{1}{2} \tilde{a}_{j,\omega}^{mn}(y) \partial_m \partial_n + \tilde{b}_{j,\omega}^m(y) \partial_m, \quad y = \varphi_{j,\omega}(x).$$

Sketch of Proof — Step 2

Parametrix Heat Kernel

Step 2a: What is a Parametrix?

Let $p_{t,\omega}^{(0)}(x, y)$ be the heat kernel of the *anchoring* operator $\frac{1}{2} \Delta_{g_\omega}$ on $(\mathcal{M}_\omega, g_\omega)$, i.e.

$$(\partial_t - \frac{1}{2} \Delta_{g_\omega})_y p_{t,\omega}^{(0)}(x, y) = 0, \quad \lim_{t \downarrow 0} p_{t,\omega}^{(0)}(x, \cdot) = \delta_x.$$

We use $p^{(0)}$ as the zeroth-order approximation and treat the rest of \mathcal{L}_ω as a perturbation.

Sketch of Proof — Step 2

Step 2a: What is a Parametrix?

Using Duhamel's (Levi/Neumann) trick,

$$(\partial_t - \mathcal{L}_\omega) p_{t,\omega}^{(0)}(x, y) = q_{t,\omega}(x, y), \quad q_{t,\omega} := (\mathcal{L}_\omega - \frac{1}{2}\Delta_{g_\omega}) p_{t,\omega}^{(0)}.$$

Treat $q_{t,\omega}$ as a source term; the genuine heat kernel solves

$$p_{t,\omega} = p_{t,\omega}^{(0)} + \int_0^t p_{t-s,\omega}^{(0)} * q_{s,\omega} \, ds,$$

whose iterates give

$$p_{t,\omega} = \sum_{n=0}^{\infty} p_{t,\omega}^{(n)}, \quad p_{t,\omega}^{(n+1)} = p_{t,\omega}^{(0)} * [(\mathcal{L}_\omega - \frac{1}{2}\Delta_{g_\omega}) p_{\cdot,\omega}^{(n)}].$$

Sketch of Proof — Step 2

Step 2b: Why the Series Converges (Uniformly)

We work in the Banach space $X := L^\infty([0, T] \times \mathcal{M}_\omega \times \mathcal{M}_\omega)$ and write the convolution operator

$$(\mathcal{K}_\omega \phi)_t(x, y) := \int_0^t \int_{\mathcal{M}_\omega} p_{t-s, \omega}^{(0)}(x, z) (\mathcal{L}_\omega - \frac{1}{2}\Delta_{g_\omega})_z \phi_s(z, y) \, d\text{vol}_{g_\omega}(z) \, ds.$$

- $p_{t-s, \omega}^{(0)}$ is the heat kernel of $\frac{1}{2}\Delta_{g_\omega}$ (smoothing).
- $(\mathcal{L}_\omega - \frac{1}{2}\Delta_{g_\omega})_z$ measures coefficient variation at z .
- $\phi_s(z, y)$ is a candidate two-point kernel at time s (for us, $\phi = p^{(n)}$).

Sketch of Proof — Step 2

Step 2b: Why the Series Converges (Uniformly)

Uniform Estimates (Valid for all $0 < t \leq T$, $x, y \in \mathcal{M}_\omega$)

(A) Gaussian bounds for $p^{(0)}$ (bounded geometry):

$$C^{-1} t^{-d/2} e^{-\frac{d_{g_\omega}(x,y)^2}{Ct}} \leq p_{t,\omega}^{(0)}(x,y) \leq C t^{-d/2} e^{-\frac{d_{g_\omega}(x,y)^2}{C^{-1}t}}.$$

(B) Coefficient-variation bound:

$$\left| (\mathcal{L}_\omega - \frac{1}{2}\Delta_{g_\omega}) p_{t,\omega}^{(0)}(x,y) \right| \leq C t^{-1} p_{ct,\omega}^{(0)}(x,y).$$

(C) Local volume comparability (small r): for $0 < r \leq r_0$, $\text{Vol}_{g_\omega}(B_r(x)) \leq C r^d$.

Sketch of Proof — Step 2

Step 2b: Why the Series Converges (Uniformly)

Using (A) to dominate $p^{(0)}$, (B) to control the integrand's "error" term, and (C) to bound the space-integral volume, we obtain

$$\|\mathcal{K}_\omega\|_{L^\infty \rightarrow L^\infty} \leq C T^\alpha, \quad \text{for some } \alpha > 0 \text{ (independent of } \omega\text{)} \implies \mathcal{K}_\omega \text{ is a } \textit{bounded} \text{ linear operator.}$$

Choosing $T > 0$ so small that $\|\mathcal{K}_\omega\| < 1$, the inverse of $\text{Id} - \mathcal{K}_\omega$ has the convergent *Neumann series*

$$(\text{Id} - \mathcal{K}_\omega)^{-1} = \sum_{n=0}^{\infty} \mathcal{K}_\omega^n, \quad \text{which is exactly } p_{t,\omega} = \sum_{n=0}^{\infty} p_{t,\omega}^{(n)}.$$

Intuitively: $p^{(0)}$ is a first guess, $\mathcal{K}_\omega p^{(0)}$ corrects for coefficient variation once, $\mathcal{K}_\omega^2 p^{(0)}$ corrects the correction, with geometric decay in operator norm guaranteeing that the sum converges uniformly.

Outcome: The series $\sum_n p_{t,\omega}^{(n)}(x, y)$ converges uniformly on $[0, T] \times \mathcal{M}_\omega \times \mathcal{M}_\omega$, yielding a genuine heat kernel $p_{t,\omega}$. This kernel then drives the tightness and martingale identification in Steps 3–5.

Sketch of Proof — Step 3

Tightness of Approximating Diffusions

- Cover \mathcal{M}_ω by normal coordinate balls $\{U_j\}_{j \in \mathbb{N}}$ of radius $r_0/4$ and take a partition of unity $\{\chi_j\}_j$ with $\text{supp } \chi_j \subset U_j$.
- Solve the SDE for $X^{(\varepsilon)}$ with coefficients $a^{(\varepsilon)}, b^{(\varepsilon)}$, stopped upon leaving a large compact set (to avoid boundary issues).
- Heat-kernel bounds yield, for each $q \geq 2$,

$$\mathbb{E} \left[d_{g_\omega}(X_t^{(\varepsilon)}, X_s^{(\varepsilon)})^q \right] \leq C |t - s|^{q/2},$$

with constants independent of ε . Kolmogorov–Chentsov $\Rightarrow \{X^{(\varepsilon)}\}_\varepsilon$ is tight in $C([0, T], \mathcal{M}_\omega)$.

Sketch of Proof — Step 4

From Tightness to A.S. Convergence

- Prohorov's theorem gives a subsequence $X^{(\varepsilon_k)} \Rightarrow X$ in law.
- Skorokhod representation theorem: on a new probability space $(\tilde{\Omega}, \tilde{\mathbb{P}})$ one can construct copies $\tilde{X}^{(\varepsilon_k)}, \tilde{X}$ such that

$$\tilde{X}^{(\varepsilon_k)} \xrightarrow{k \rightarrow \infty} \tilde{X} \quad \text{almost surely in } C([0, T], \mathcal{M}_\omega).$$

This a.s. limit is the candidate diffusion for the true coefficients a_ω, b_ω .

The almost-sure convergence lets us pass Itô/martingale identities term-by-term in Step 5, finishing the weak-existence proof.

Sketch of Proof — Step 5

Martingale Identification

Step 5a: From the SDE Coefficients to a Martingale

For each point $x \in \mathcal{M}_\omega$ let

$$\sigma_\omega(x) : \mathbb{R}^m \longrightarrow T_x \mathcal{M}_\omega$$

be a linear map that pushes an m -dimensional Euclidean Brownian increment dW_t into the tangent space $T_x \mathcal{M}_\omega$.

In local coordinates $x = (x^1, \dots, x^d)$ we can write

$$\sigma_{\omega,k}^i(x) = [\sigma_\omega(x)]_k^i, \quad 1 \leq i \leq d, 1 \leq k \leq m.$$

The associated *diffusion matrix* is

$$a_\omega^{ij}(x) = \sum_{k=1}^m \sigma_{\omega,k}^i(x) \sigma_{\omega,k}^j(x),$$

so $a = \sigma \sigma^*$ and σ is a “matrix square-root” of a .

B

Sketch of Proof — Step 5

Step 5a: From the SDE Coefficients to a Martingale

Given the SDE

$$dX_t = \sigma_\omega(X_t) dW_t + b_\omega(X_t) dt,$$

and any $f \in C^2(\mathcal{M}_\omega)$,

$$f(X_t) = f(X_0) + \underbrace{\int_0^t \nabla f(X_s) \sigma_\omega(X_s) dW_s}_{\text{local martingale}} + \underbrace{\int_0^t \left[\frac{1}{2} \operatorname{tr}(\sigma_\omega \sigma_\omega^* \nabla^2 f) + b_\omega \cdot \nabla f \right](X_s) ds}_{(\mathcal{L}_\omega f)(X_s)}$$

Subtract $f(X_0)$ and the drift integral:

$$M_t(f) := f(X_t) - f(X_0) - \int_0^t \mathcal{L}_\omega f(X_s) ds \quad \text{is a martingale.}$$

Sketch of Proof — Step 5

Step 5b: Applying Itô to the Processes

For each $\varepsilon > 0$,

$$M_t^{(\varepsilon)}(f) := f(X_t^{(\varepsilon)}) - f(X_0^{(\varepsilon)}) - \int_0^t \mathcal{L}_\omega^{(\varepsilon)} f(X_s^{(\varepsilon)}) \, ds \quad \text{is a martingale.}$$

Heat-kernel and coefficient estimates give

$$\sup_{\varepsilon} \mathbb{E} \int_0^T |\mathcal{L}_\omega f - \mathcal{L}_\omega^{(\varepsilon)} f|(X_s^{(\varepsilon)}) \, ds \longrightarrow 0.$$

Together with a.s. convergence $X^{(\varepsilon_k)} \rightarrow X$ (Step 4) and

$$\sup_{\varepsilon} \mathbb{E} \left[\sup_{t \leq T} |M_t^{(\varepsilon)}(f)| \right] < \infty \quad (\text{BDG + bounded coefficients}),$$

the family $\{M^{(\varepsilon)}(f)\}_{\varepsilon}$ is uniformly integrable, so the L^1 limit

$$M_t(f) := f(X_t) - f(X_0) - \int_0^t \mathcal{L}_\omega f(X_s) \, ds \quad \text{is a martingale for every } f \in C_c^\infty(\mathcal{M}_\omega).$$

Sketch of Proof — Conclusion

Conclusion

The limiting process X_t solves the martingale problem $(\mathcal{L}_\omega, \delta_x)$. Hence weak existence holds for all $x \in \mathcal{M}_\omega$ under bounded geometry. Moreover, under our $C^{2,\alpha}$ coefficients and uniform ellipticity, **uniqueness in law** follows from the Stroock–Varadhan theory for the martingale problem.

Strong Solutions on a Random Stage

- **Strong/pathwise solution.** Fix a *single* filtered space $(\Omega, \mathcal{F}, (\mathcal{F}_t), \mathbb{P})$ carrying a d -dimensional Brownian motion W_t that is independent of the geometry. We seek an (\mathcal{F}_t) -adapted process X_t on \mathcal{M}_ω satisfying

$$dX_t = \sigma_\omega(X_t) dW_t + b_\omega(X_t) dt, \quad X_0 = x,$$

without adding new randomness.

- **Pathwise uniqueness.** If X_t and X'_t solve the same SDE with the same W_t and start at x , then $\mathbb{P}(X_t = X'_t \ \forall t) = 1$.
- **Yamada–Watanabe (classical).** In \mathbb{R}^d : *strong \Leftrightarrow weak + pathwise uniqueness*. The proof relies on: (i) coupling any two weak solutions on the same space, (ii) Itô's formula for $|X_t - X'_t|^2$.
- **Open question.** Can one replicate Yamada–Watanabe when both the metric g_ω and the coefficients $(\sigma_\omega, b_\omega)$ are *random* and vary with ω ?

Why Pathwise Results Remain Open

- (A) **No canonical noise.** Brownian motion on $(\mathcal{M}_\omega, g_\omega)$ is defined via the Laplace–Beltrami operator of that metric. To compare two geometries ω and ω' you must lift both to a common frame bundle and synchronise their stochastic parallel transports—a measurable selection of such a coupling is still unknown.
- (B) **Cut-locus explosions.** The squared distance function $d_{g_\omega}^2(\cdot, \cdot)$ loses C^2 -smoothness when geodesics bifurcate. Itô's formula for $d^2(X_t, X'_t)$, central in the classical proof of pathwise uniqueness, thus breaks down beyond the first cut-locus hitting time—and that time can be arbitrarily small for a set of ω of full measure.
- (C) **Geometry-driven irregular coefficients.** Even if (σ, b) are $C^{2,\alpha}$ on each fixed manifold, the family $\{\sigma_\omega\}_\omega$ may be only measurable in ω . Hence global Sobolev norms fail to be uniform, thwarting Picard iterations that require Lipschitz bounds simultaneously for all ω .
- (D) **Filtration mismatch.** The σ -algebra generated by the geometry often strictly contains the one generated by (W_t) , so $\sigma(W_s : 0 \leq s \leq t) \not\supseteq \sigma(\mathcal{M}_\omega)$. Classical strong solutions assume the opposite inclusion.

Thank you!

Questions, comments, or thoughts?